AGU
ADVANCING
EARTH AND
SPACE SCIENCE

Geophysical Research Letters

Key Points:
- Lockdown restrictions during COVID-19 have reduced emissions of aerosols and greenhouse gases
- 12 CMIP6 Earth system models have performed coordinated experiments to assess the impact of this on climate
- Aerosol amounts are reduced over southern and eastern Asia but there is no detectable change in annually averaged temperature or precipitation

The Climate Response to Emissions Reductions Due to COVID-19: Initial Results From CovidMIP

Chris D. Jones[1], Jonathan E. Hickman[2], Steven T. Rumbold[3], Jeremy Walton[1], Robin D. Lamboll[4], Ragnhild B. Skeie[5], Stephanie Fiedler[6,7], Piers M. Forster[8], Joeri Rogelj[4,9], Manabu Abe[10], Michael Botzet[11], Katherine Calvin[12,13], Christophe Cassou[14], Jason N. S. Cole[15], Paolo Davini[16], Makoto Deushi[17], Martin Dix[18], John C. Fyfe[15], Nathan P. Gillett[15], Tatiana Ilyina[11], Michio Kawamiya[10], Maxwell Kelley[19,2], Slava Kharin[15], Tsuyoshi Koshiro[17], Hongmei Li[11], Chloe Mackallah[18], Wolfgang A. Müller[11], Pierre Nabat[20], Twan van Noije[21], Paul Nolan[22,23], Rumi Ohgaito[10], Dirk Olivié[24], Naga Oshima[17], Jose Parodi[25], Thomas J. Reerink[21], Lili Ren[26], Anastasia Romanou[2], Roland Séférian[20], Yongming Tang[1], Claudia Timmreck[11], Jerry Tjiputra[27], Etienne Tourigny[28], Kostas Tsigaridis[29,2], Hailong Wang[12], Mingxuan Wu[12], Klaus Wyser[30], Shuting Yang[31], Yang Yang[26], and Tilo Ziehn[18]

[1]Met Office Hadley Centre, Exeter, UK, [2]NASA Goddard Institute for Space Studies, New York, NY, USA, [3]National Centre for Atmospheric Science, University of Reading, UK, [4]Grantham Institute for Climate Change and the Environment, Imperial College London, London, UK, [5]CICERO Center for International Climate Research, Oslo, Norway, [6]Institute of Geophysics and Meteorology, University of Cologne, Cologne, Germany, [7]Climate Monitoring and Diagnostics, Hans-Ertel-Centre for Weather Research, Bonn/Cologne, Germany, [8]Priestley International Centre for Climate, University of Leeds, UK, [9]International Institute for Applied Systems Analysis (IIASA), Laxenburg, Austria, [10]Japan Agency for Marine-Earth Science and Technology, Yokohama, Japan, [11]Max Planck Institute for Meteorology, Hamburg, Germany, [12]Pacific Northwest National Laboratory, Richland, WA, USA, [13]Pacific Northwest National Laboratory, College Park, MD, USA, [14]CECI, CNRS, CERFACS, Université de Toulouse, Toulouse, France, [15]Canadian Centre for Climate Modelling and Analysis, Environment and Climate Change Canada, Victoria, BC, Canada, [16]Istituto di Scienze dell'Atmosfera e del Clima, Consiglio Nazionale delle Ricerche (CNR-ISAC), Torino, Italy, [17]Meteorological Research Institute, Japan Meteorological Agency, Tsukuba, Japan, [18]CSIRO Oceans and Atmosphere, Aspendale, VIC, Australia, [19]SciSpace LLC, New York, NY, USA, [20]CNRM, CNRS, Université de Toulouse, Toulouse, France, [21]Royal Netherlands Meteorological Institute (KNMI), AE De Bilt, Netherlands, [22]Irish Centre for High-End Computing (ICHEC), I, Trinity Technology & Enterprise Campus, Dublin 2, Ireland, [23]Met Éireann, Research and Applications Division, Dublin, Ireland, [24]NORCE Norwegian Meteorological Institute, Oslo, Norway, [25]Spanish State Meteorological Agency (AEMET), Murcia, Spain, [26]Jiangsu Key Laboratory of Atmospheric Environment Monitoring and Pollution Control, Jiangsu Collaborative Innovation Center of Atmospheric Environment and Equipment Technology, School of Environmental Science and Engineering, Nanjing University of Information Science and Technology, Nanjing, China, [27]Norwegian Research Centre and Bjerknes Centre for Climate Research, Bergen, Norway, [28]Earth Sciences Department, Barcelona Supercomputing Center (BSC), Barcelona, Spain, [29]Center for Climate Systems Research, Columbia University, New York, NY, USA, [30]Rossby Centre, Swedish Meteorological and Hydrological Institute (SMHI), Norrköping, Sweden, [31]Danish Meteorological Institute (DMI), Copenhagen, Denmark

Abstract Many nations responded to the corona virus disease-2019 (COVID-19) pandemic by restricting travel and other activities during 2020, resulting in temporarily reduced emissions of CO_2, other greenhouse gases and ozone and aerosol precursors. We present the initial results from a coordinated Intercomparison, CovidMIP, of Earth system model simulations which assess the impact on climate of these emissions reductions. 12 models performed multiple initial-condition ensembles to produce over 300 simulations spanning both initial condition and model structural uncertainty. We find model consensus on reduced aerosol amounts (particularly over southern and eastern Asia) and associated increases in surface shortwave radiation levels. However, any impact on near-surface temperature or rainfall during 2020–2024 is extremely small and is not detectable in this initial analysis. Regional analyses on a finer scale, and closer attention to extremes (especially linked to changes in atmospheric composition and air quality) are required to test the impact of COVID-19-related emission reductions on near-term climate.

Plain Language Summary Many nations responded to the COVID-19 pandemic by restricting travel and other activities during 2020. This caused a temporary reduction in emissions of CO2 and other pollutants. We compare results from twelve Earth system models to see if the emissions

reductions affected climate. These twelve models performed over 300 experiments using multiple initial-conditions. We find a consensus that aerosol amounts were reduced, especially over southern and eastern Asia, during 2020-2024. This led to increases in solar radiation reaching the surface in this region. However, we could not detect any associated impact on temperature or rainfall. We recommend more analyses on regional scales. We also suggest that analysis of extreme weather and air quality would be useful to test the impact on climate of emission reductions due to COVID-19.

1. Introduction

1.1. Impact of COVID-19 Lockdown on Emissions

The corona virus disease-2019 (COVID-19) pandemic led to widespread measures restricting travel, industrial, and commercial activity during 2020. The effects of these changes in socioeconomic activity on atmospheric composition have been widely studied including estimates of emissions and concentrations of species that directly or indirectly affect climate.

The impacts of COVID-19 measures on long-lived greenhouse gases have been inferred from both bottom-up estimates using activity data and top-down analysis of atmospheric observations. Bottom-up estimates using sector activity have estimated global CO_2 emissions reductions of 8.8% during the first 5 months of 2020 (Liu et al., 2020) and annual reductions from 4% to 7% (Le Quéré et al., 2020). Top-down assessments have found some indications of a decrease in CO_2 growth rate during 2020 (Buchwitz et al., 2020), with examples of substantial local and regional CO_2 and methane (CH_4) emissions reductions inferred from surface observations (Tohjima et al., 2020; Turner et al., 2020). However, existing satellite products could not provide the required coverage to reliably detect changes in CO_2 column densities at the magnitude expected to be occurring in 2020 (Buchwitz et al., 2020; Chevallier et al., 2020). Expected growth rates in atmospheric CO_2 fractions vary too much from year to year due to internal climate variability (Betts et al., 2016; Jones and Cox, 2005) for the effects of emission reductions on the order of 8% to be clearly detected from observations of CO_2 column densities (Sussmann & Rettinger, 2020; Tohjima et al., 2020). The long lifetime of CO_2, and to a lesser extent CH_4, means that the small impact of emissions reductions is likely to be long-lived, and may still exert a non-negligible climate impact on decadal timescales (Forster et al., 2020).

The largest changes in observed composition attributed to COVID-19 restrictions were for nitrogen dioxide (NO_2), with concentration reductions at both national- and city-scales typically on the order of 20%–60% in China, India, Europe, and the United States (Goldberg et al., 2020; Keller et al., 2020; Menut et al., 2020; Miyazaki et al., 2020; Ordóñez et al., 2020; Venter et al., 2020; Zhao et al., 2020). The NO_2 decreases have been attributed largely to changes in the transport sector (Bao & Zhang, 2020; Diamond & Wood, 2020; Lian et al., 2020; Venter et al., 2020). The rapid changes in emissions and complex dynamics of short-lived pollutants have complex and non-uniform implications for climate. In areas where background NO_x concentrations were high, reduced NO_x emissions led to increased tropospheric ozone (O_3) concentrations in many regions and cities (Keller et al., 2020; Le et al., 2020; Lian, Huang, Huang, et al., 2020; Ordóñez et al., 2020; Sicard et al., 2020; Venter et al., 2020). Elsewhere, tropospheric ozone may have decreased during lockdowns leading to short-term estimated changes of radiative forcing by -33 to -78 m Wm^{-2} (Weber et al., 2020).

Some studies report substantial decreases in particulate matter (PM) on the order of 10%–30% (Filonchyk et al., 2020; Le et al., 2020; Silver et al., 2020; Venter et al., 2020; Xu et al., 2020), but analyses accounting for long-term trends generally found no lockdown impacts on aerosol optical depth (AOD) or PM concentrations (Diamond & Wood, 2020; Field et al., 2020; Zangari et al., 2020). In some regions, PM concentrations increased as a result of altered dust or biomass burning emissions or as a consequence of changes in emissions and meteorology (Le et al., 2020; Venter et al., 2020). Notably, northern China experienced an increase in haze during the spring lockdown due to enhanced formation of ozone, which, in combination with favorable meteorological conditions and changes in heterogeneous chemistry, contributed to enhanced secondary aerosol formation (Chang et al., 2020; Le et al., 2020; Wang et al., 2020b).

1.2. Impact of Emissions Reductions on Climate

The reduction in emissions is expected to have regional impacts on atmospheric composition, and therefore could have implications for weather and climate. Different species have very different lifetimes from hours-to-days for aerosols, to decades or longer for long-lived greenhouse gases, and very different spatial scales, with some being very localized and others globally well-mixed.

For example, Yang et al. (2020) examined climate responses to aerosol emission reductions during the COVID-19 lockdown, back-to-work and post-lockdown stages throughout the year 2020 based on CESM1 model simulations. They reported that an anomalous surface warming appeared over the Northern Hemisphere continents due to the fast climate response to aerosol reductions. Forster et al. (2020) developed a two-year COVID-19 emissions reduction scenario for long- and short-lived species based on mobility data and the bottom-up approach of Le Quéré et al. (2020) for some sectors and then assumed a recovery over the subsequent two years. Using the FaIR climate emulator, they simulated the effect of these emissions reductions and found a rapid short-term warming due to reduced aerosols, which was offset by a slightly slower, but also near-term cooling due to reduced tropospheric ozone. On longer timescales, well-mixed GHGs, especially CO_2 became important, and their simulations showed that the net effect of these emissions changes by 2030 was negligible: a global cooling of about 0.01 ± 0.005°C.

However, because FaIR cannot capture regional climate effects, internal variability or complex interactions of atmospheric composition and biogeochemistry, there remain unanswered questions about the possible climatic impact of emissions reductions on regional air quality and climate. These are beginning to be addressed by single model studies (e.g., Yang et al., 2020 analyze an atmospheric model with prescribed sea surface temperature), but would benefit greatly from being analyzed across an ensemble of Earth system models (ESMs) run under a common protocol. Hence it was decided that this scenario would form the basis of a multi-Earth system model intercomparison project (MIP). This paper presents an initial analysis of the first results coming from this new activity, called CovidMIP. The emissions estimates and modeling protocol used are described in Section 2, results shown in Section 3 and discussed in Section 4 in the context of ongoing climate change.

2. Materials and Methods

2.1. CovidMIP Protocol

The emissions estimates assembled by Forster et al. (2020) were collated and gridded, and made available in Inputs4MIPs data format for use by CMIP Earth system models (Lamboll et al., 2020). A modeling protocol was agreed, and is incorporated into DAMIP (the Detection and Attribution MIP; Gillett et al., 2016), which is also described in Lamboll et al. (2020), but the main points are noted here for convenience.

Because any climate signal due to COVID-19-induced emissions reductions was considered likely to be small, it is advantageous to carry out large initial-condition ensembles which have been shown to enable detection of even small regional climate signals (e.g., Banerjee et al., 2020). But cognizant of the computational cost and time required for producing such large ensembles, a pragmatic recommendation was made that model groups perform at least 10 initial-condition ensemble members. This was hoped to maximize the number of modeling groups participating but still produce enough members to enable meaningful analysis.

The protocol uses the SSP2-4.5 scenario (O'Neill et al., 2016) as a baseline against which to apply the emissions reductions. Simulations are run parallel to ssp245, but branching from that simulation on January 1, 2020 and following the new forcing in line with emissions reductions. The results will be published on the CMIP6 archive (Earth System Grid Federation) under experiment name ssp245-covid. Forcing is provided as concentrations of greenhouse gases and emissions of aerosols and aerosol and ozone precursors. For models with interactive chemistry, ozone can be simulated otherwise it has been provided as concentrations. Similarly, models can simulate aerosols or they can be represented with the MACv2-SP parametrization (Fiedler et al., 2020; Stevens et al., 2017).

In this manuscript we focus on the immediate term impact (from 2020 to 2024) of the "two year blip" scenario under which emissions revert to the baseline levels by the end of 2022. In addition to this, Forster et al. (2020) created a set of scenarios spanning possible future economic recovery strategies: a reduction in

anthropogenic CO_2 emissions post-2020 consistent with enhanced investment in environmentally friendly technologies (moderate or strong "green stimulus"), no effect after 2022 (continuation of "two year blip" studied here with emissions reverting to ssp245) or an increase in anthropogenic CO_2 emissions relative to ssp245 after 2020 consistent with an investment in more traditional fossil-fuel based energy production (or "fossil-fueled recovery"). All of these scenarios have become part of the CMIP6 set of experiments, under the detection and attribution activity (DAMIP: Gillett et al., 2016).

2.2. Participating Earth System Models

The protocol is open to all models participating in CMIP6 and to date 12 models have provided data for analysis (Table 1). A particular value of a multi-model ensemble is being able to incorporate different levels of process complexity, but this also brings challenges of interpreting results.

Some models prescribe aerosols and ozone, either using their own climatology or MACv2-SP and/or prescribed ozone 3D concentrations taken from the OsloCTM3 chemical transport model (Lamboll et al., 2020). Others may simulate either aerosols or ozone interactively in response to their primary or secondary emissions. The MPI -ESM1-2-LR model simulated interactive CO_2 while the other models used prescribed CO_2 concentrations. Models have differing complexity and species richness of aerosols, representing both natural and anthropogenic species such as sulfates, black carbon, organic carbon, sea-salt, and mineral-dust, but many still lack representation of nitrate aerosols.

In terms of biogeochemistry many ESMs now represent land and marine ecosystems and the carbon cycle (Boysen et al., 2020; Séférian et al., 2020; Thornhill et al., 2020). On the near-term studied here, the carbon cycle is unlikely to have a large effect on climate but impacts of emissions reductions may show up in terms of changes in carbon fluxes, stores and partitioning across realms of the Earth system.

To generate initial conditions some models (ACCESS-ESM1-5, CanESM5, EC-Earth3, MIROC-ES2L, MPI-ESM1-2-LR, UKESM1-0-LL) drew on existing ssp245 simulations which followed on from initial-condition ensembles of the CMIP6 historical simulations. Others perturbed conditions at the end of the historical period (CESM1, E3SM-1-1, GISS-E2-1-G), or mixed the two approaches by inflating existing ensembles with additional perturbations applied (MRI-ESM2-0, CNRM-ESM2-1, NorESM2-LM) or by running on different super-computers (NorESM2-LM).

Future studies will be able to take into account the model complexity and how this affects the simulated results. For example, are changes in atmospheric circulation or surface climate affected differently between models with simulated and prescribed ozone and aerosols? How does the model treatment of interactions between atmospheric composition (such as fraction of diffuse light or surface ozone) affect vegetation productivity and carbon storage? In this analysis such considerations are out of scope and we give an overview on each model's results for the climate response for 2020–2024. The reader is referred to Table 1, which documents the spatial resolution and the process complexity of each participating model as well as the number of ensemble members utilized in this study.

3. Results

3.1. Indicators of Global Change

Our analysis draws on different sized ensembles from 12 ESMs. Throughout, we base analysis on ensemble mean anomalies from each model, calculated from a pair-wise difference between simulations with COVID-19-related emissions reductions ("ssp245-covid") and simulations using the standard, baseline SSP2-4.5 scenario ("ssp245").

Globally, for 2020, all models show a reduction in aerosol optical depth (at 550 nm) in their ensemble mean with seven out of 11 models which reported this variable having a reduction greater than one standard deviation (Figure 1). In 2021, the AOD anomalies of 10 out of 11 models remain negative with ACCESS-ESM1-5 showing near-zero deviation. From 2022 onwards there is no robust global signal in AOD as emissions reductions in this simulation recover to levels in the baseline scenario and aerosol amounts quickly recover too.

Table 1
List of Participating Models, Their Main Properties and Number of Ensemble Members Used in This Study

Model name	Reference	Atmosphere resolution [a]	Ocean resolution [a]	ssp245-covid ensemble members	Aerosol processes [b]	Ozone forcing	Aerosol forcing
ACCESS-ESM1-5	Ziehn et al. (2020)	250 km (N96), L38	100 km, L50	30		5; CLASSIC	interactive
CanESM5	Swart et al. (2019)	500 km (T63), L49	100 km, L45	50		5; Parameterized using a prognostic scheme for bulk concentrations	interactive
CESM1	Hurrell et al. (2013)	250 km (1.9 × 2.5), L30	100 km (gx1v6), L60	10		6; MAM4	interactive
CNRM-ESM2-1	Séférian et al. (2019)	250 km (TL127,1.4°), L91	100 km (eORCA1), L75	100		5; TACTIC (Michou et al., 2020)	interactive
E3SM-1-1	Burrows et al. (2020)	100 km (NE30), L72	60–30 km, L100	10		7; MAM4 (Wang et al., 2020a)	interactive
EC-Earth3	(Döscher, R. et al., 2021)	100 km (T255), L91	100 km (eORCA1), L75	30		n/a	MACv2-SP (Fiedler et al., 2020)
MIROC-ES2L	Hajima et al. (2020); Kawamiya et al. (2020)	500 km (T42), L40	100 km (360 × 256), L63	30		5; SPRINTARS	interactive
MPI-ESM1-2-LR	Mauritsen et al. (2019)	250 km (T63), L47	150 km, L40	10		n/a	MACv2-SP (Fiedler et al., 2020)
MRI-ESM2-0	Yukimoto et al. (2019); Oshima et al. (2020)	100 km (TL159, 1.125°), L80	100 km (tripolar 1° x 0.3° −0.5°), L61	10		5; MASINGAR mk-2r4c	interactive
GISS-E2-1-G	Kelley et al., 2020; Ito et al., 2020; Bauer et al., 2020	250 km (2 × 2.5°), L40	100 km (1 × 1.25°), L40	10		8; MATRIX	interactive
NorESM2-LM	Seland et al. (2020); Tjiputra et al. (2020)	250 km (1.9° x 2.5°), L32	100 km, L53	10		5; OsloAero6	interactive
UKESM1-0-LL	Sellar et al. (2019)	250 km (N96), L85	100 km (eORCA1), L75	16		5; UKCA MODE	interactive

[a]shown as CMIP "nominal resolution" in km, "L" denotes number of vertical levels. Grid name or information provided if available. [b]number of aerosol species, and name/description of aerosol sub-model. [c]These models used the first version of the ozone fields that had a small bug in the vertical interpolation of the ozone perturbation, stretching the ozone perturbation to too high altitudes. The models weres not able to re-run the model simulations with the corrected ozone fields. Radiative kernel calculations following Skeie et al. (2020) gave 0.6 mWm^{-2} stronger total ozone radiative forcing in 2020 for the corrected fields compared to the incorrect ozone fields, that are small compared to the total ozone radiative forcing of −37 m Wm^{-2} for ssp245-covid relative to ssp245 in 2020.

This behavior is reflected in the amount of solar radiation reaching the surface, which is generally simulated to have increased, with all models (of the 11 for whom this variable was available for this analysis) having a positive anomaly in downwards shortwave (SW) radiation for both 2020 and 2021 (Figure 1, panel b). Although only MRI-ESM2-0 simulated an ensemble mean global increase greater than 1 standard deviation. As for AOD, the anomaly quickly recovers and becomes very small from 2022 onwards. We have not yet investigated the extent to which surface shortwave is directly affected by aerosol absorption or by aerosol-induced changes in cloud cover. Future studies will also assess impacts and implications of aerosol-cloud interactions in driving the changes seen here.
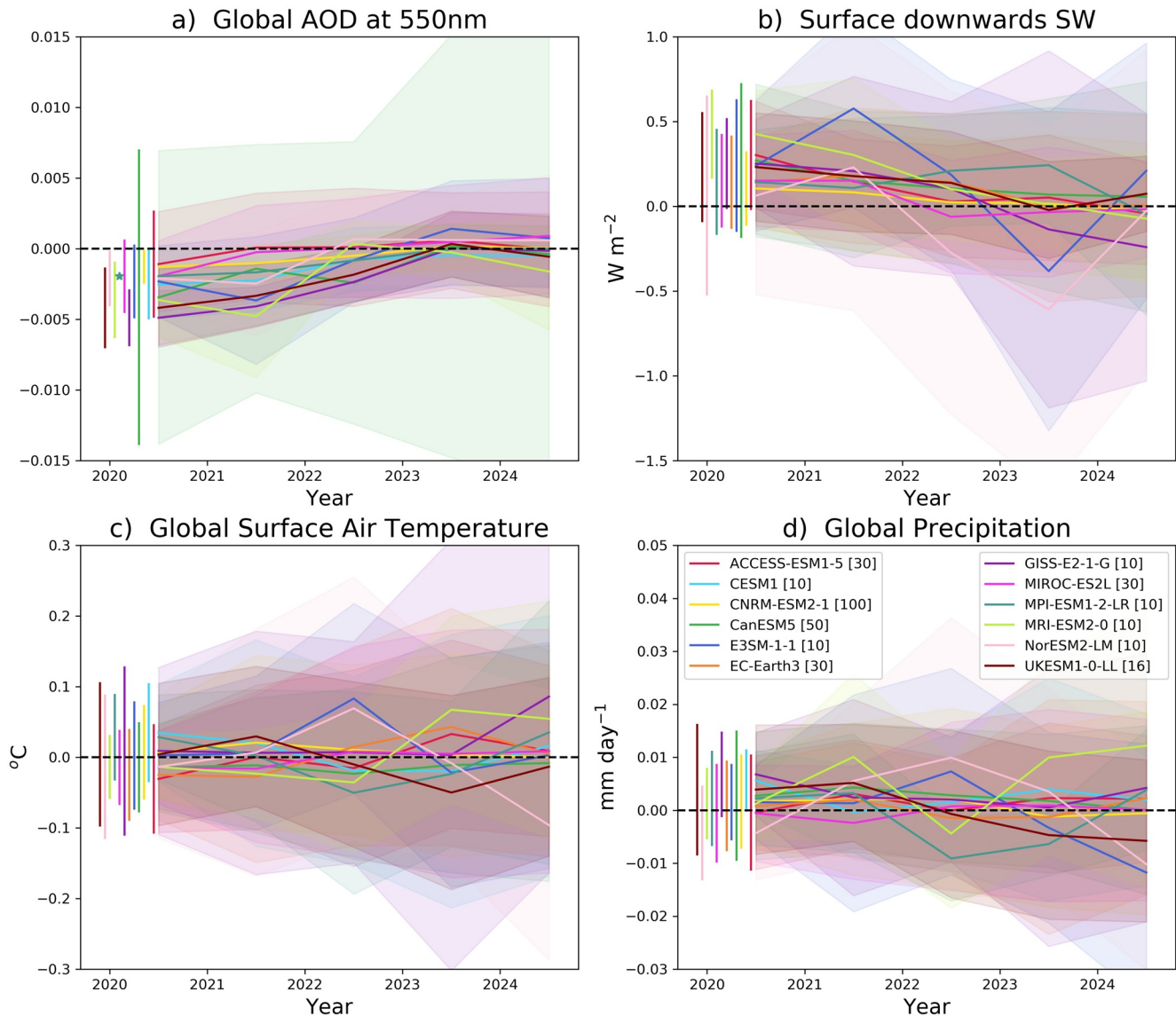
Figure 1. Annual mean, ensemble average output from ESMs. Each panel shows anomalies from the simulations with COVID-19-related emissions reductions compared to the baseline SSP2-4.5 simulations ("ssp245-covid" minus "ssp245"). (a) Global aerosol optical depth at 550 nm; (b) downwards SW radiation at the surface; (c) Global surface air temperature; (d) Global precipitation. Colored lines show ensemble average results from each model, and paler plumes show ensemble spread for each model calculated here as ±1 standard deviation across each model's ensemble. Vertical bars to the left of each panel show each model spread (mean ± 1 standard deviation) for the first year, 2020. Each model has performed a different number of ensemble members as listed in Table 1 and shown in square brackets in the caption.

The impact of this, however, on surface climate at a global scale is very small. Figures 1c and 1d show globally averaged surface air temperature and precipitation respectively. No model shows any significant change in either of these quantities at a global level for any year.

3.2. Patterns of Regional Changes

Figure 2 shows the regional patterns of the changes in aerosol optical depth for each model. It is apparent that models agree that the largest response is in Asia, predominantly over India and China where almost all models show a marked decrease in aerosols as an average over the 5-year period 2020–2024. Some models also show some patches of aerosol increases, for example CanESM and E3SM-1-1 over the Himalayan region, and MIROC-ES2L over regions of North Africa. Reasons for these changes are not explored further
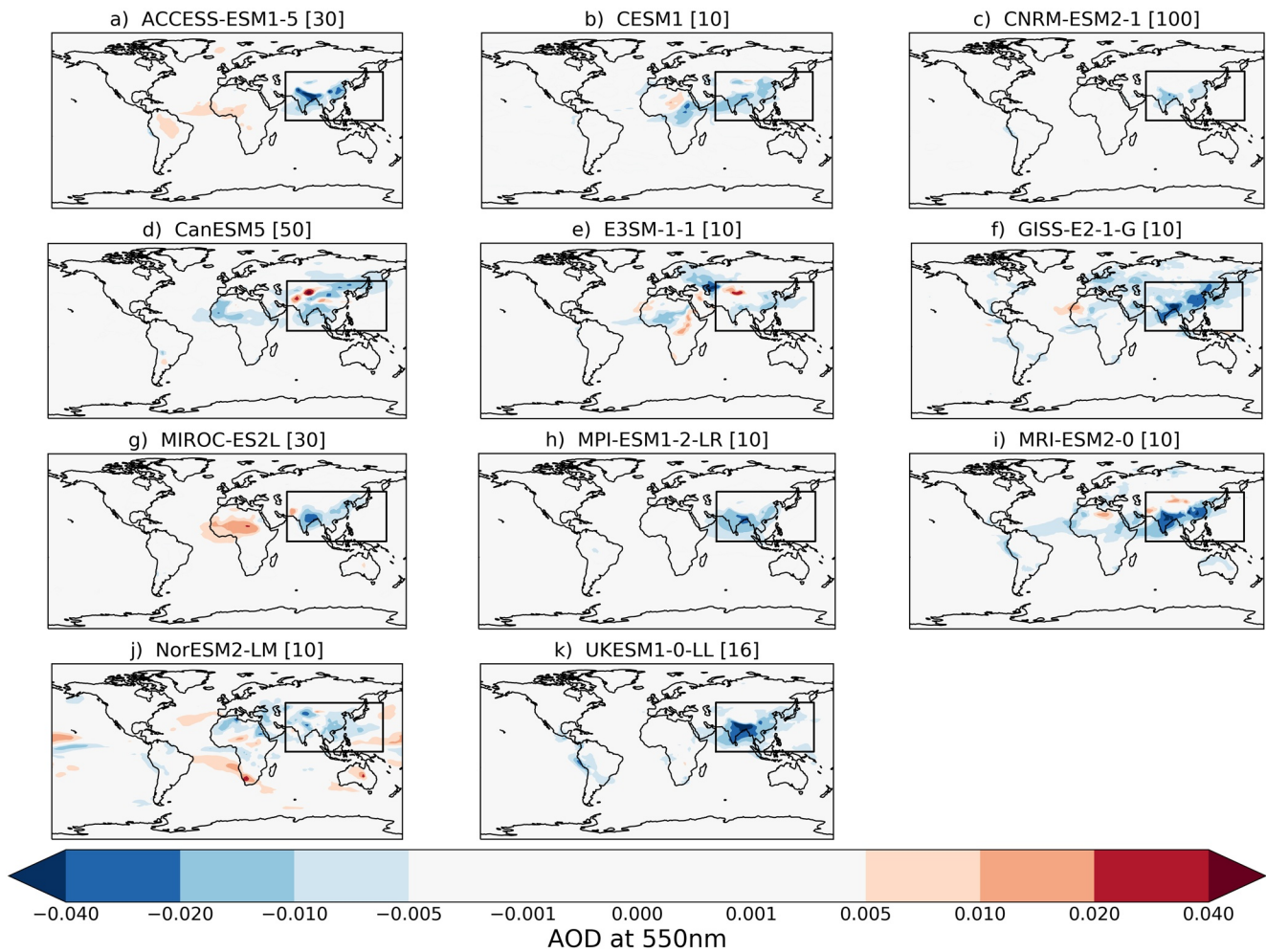
Figure 2. Model by model simulated changes in aerosol optical depth (at a wavelength of 550 nm). For each model we plot the ensemble mean response from 2020–2024 inclusive. Blue colors denote a decrease in AOD. Each model has performed a different number of ensemble members as listed in Table 1 and shown in square brackets in the caption. The black box shows the region analyzed in Figure 3.

here and we do not yet know if they are caused by changes in anthropogenic or natural sources, such as dust, which can be very sensitive to variations in windspeed.

To see if these regional changes in aerosol loading affect regional climate properties, we define a region bounded by 60–160° E and 0–50° N which has been chosen subjectively after considering all models to cover the main AOD anomalies across models (marked as black boxes in Figure 2). We assess annual changes in surface SW radiation, temperature and precipitation in this region. Figure 3 shows a similar response to the global metrics shown in Figure 1 but with greater magnitudes of average response. Again, there is a strong model agreement of reduced aerosols, with all models agreeing on this in their ensemble mean for 2020 and seven out of 11 having reductions greater than 1 standard deviation. Averaged across models, global AOD reduction in 2020 is -0.0027 ± 0.0012, while in southern and eastern Asia it is -0.0097 ± 0.0034. The associated increase in downwards SW radiation is also apparent, and stronger here: globally models show an increase of 0.21 ± 0.10 Wm^{-2} while in southern and eastern Asia it is 0.69 ± 0.31 Wm^{-2}.

Although most models simulate a slight warming signal in this region in their ensemble mean (Figure 3c), the magnitude is very small, less than 0.1 C, and in all models smaller than the standard deviation across ensemble members (typically of the order 0.2 C).

Outside of this region, models show patchy temperature changes, indicative of random changes, and internal variability of modes such as NAO or ENSO. This residual signal of internal variability is not eliminated
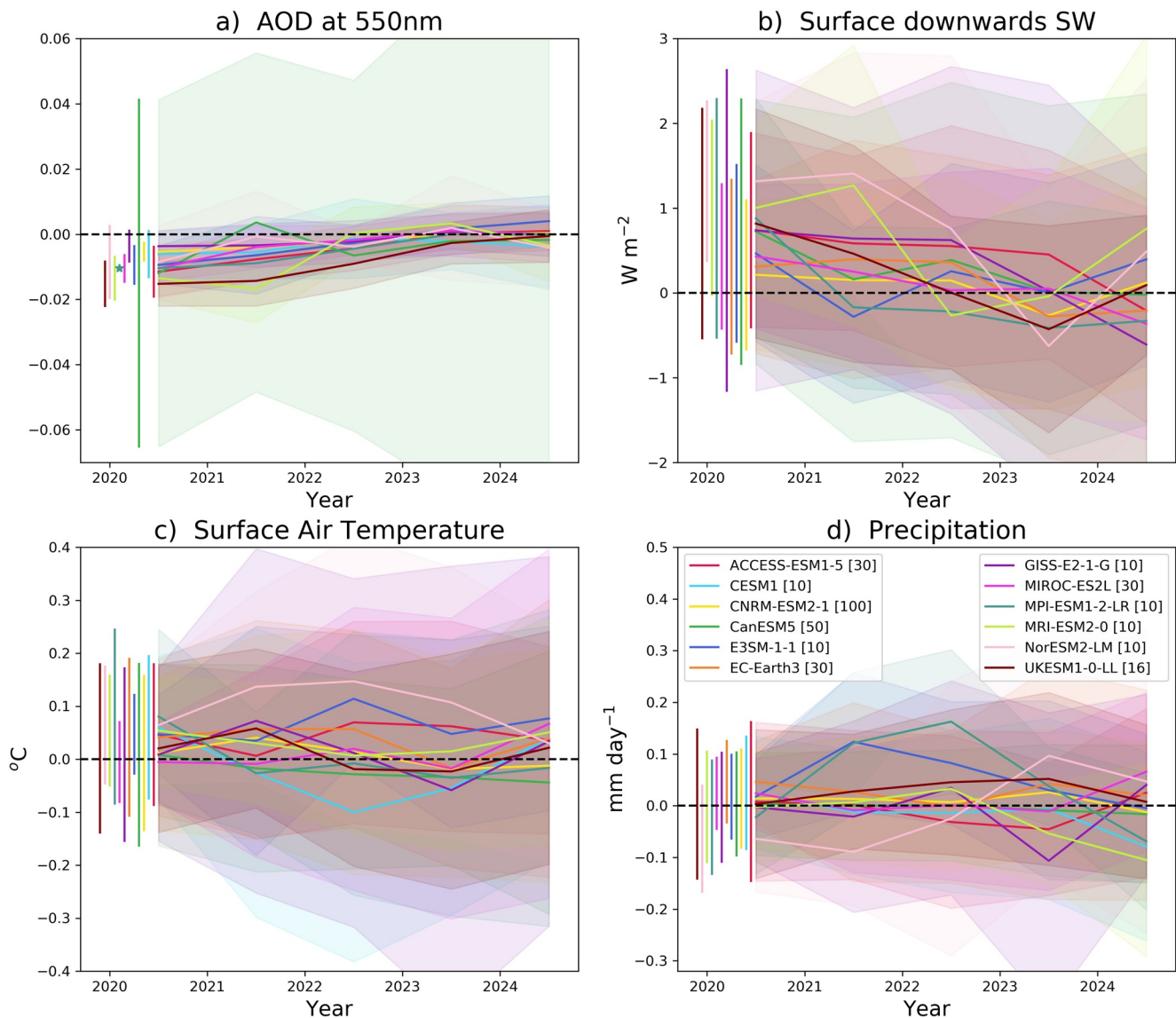
Figure 3. Indicators of change in southern and eastern Asia (defined here as 60–160° E and 0–50°N). As for Figure 1 results are plotted as annual mean anomalies, with colored lines denoting ensemble means from each model and gray shading 1-standard deviation for each model. (a) Aerosol optical depth; (b) surface downwards shortwave radiation; (c) surface air temperature; (d) precipitation.

in limited ensemble size and demonstrates the weak signal-to-noise ratio (see Figure S1 in Supplementary Info). These changes do not appear to be systematic, with some regions exhibiting both apparently strong warming and cooling signals in different models. The region of northern East Asia often displays a strong temperature signal in the model results, with CESM1 displaying a warming as reported in Yang et al. (2020), although that study performed simulations with fixed sea-surface temperatures. GISS-E2-1-G and E3SM-1-1 also show strong warming patterns here and UKESM1-0-LL, MPI-ESM1-2-LR and CanESM5 some warming too. But NorESM2-LM shows a strong cooling and ACCESS-ESM1-5, MIROC-ES2L and MRI-ESM2-0 having mixed signals. Models show marked differences elsewhere e.g. MPI-ESM1-2-LR and MRI-ESM2-0 have opposite patterns of warming over North America while in South America CanESM5 and UKESM1-0-LL show a cooling but GISS-E2-1-G and NorESM2-LM show a warming.

When looking at regional patterns of precipitation and surface SW radiation (S.I. Figures S2 and S3) there are no robust signals or consistent patterns of change across models. Even the increase in surface SW radiation shown in Figure 3 is very hard to see by eye in the patterns of change, due to the influence of clouds

which can easily mask any signal from changes in aerosols. This, and similar incoherent patterns of rainfall change, indicate the substantial variability in these quantities and the challenges in detecting robust signals of change under conditions of relatively small forcing. Despite a large number of ensembles, it is evident that at these smaller regional scales, variability in meteorology prevents robust detection of signals in clouds and rainfall.

4. Discussion and Conclusions

Here we have only begun to scratch the surface of the results becoming available from the CovidMIP simulations. We stress that this work has been the result of a very rapid response of the Earth system modeling community. It often takes several years to design and perform coordinated MIP experiments, and process the data for publication in a community archive. This activity has taken place in only a matter of months. This paper is just the very first analysis of initial results and therefore serves only as a first indication of how the climate system has responded to the perturbations to emissions in response to the COVID-19 pandemic. It is not possible at this stage to analyze all of the responses, nor the processes responsible for changes across the whole system. But this study sets the scene and informs priorities for future analysis.

We have shown that the imprint of COVID-19-related changes in societal activity is visible in atmospheric composition, notably aerosol optical depth over southern and eastern Asia, and in the amount of solar radiation reaching the planet's surface. Over this most affected region, the 2-years average effect was more than 0.5 Wm^{-2}. More locally and on shorter timescales it could be substantially higher. However, despite these changes in the make-up of the atmosphere, no detectable change in surface temperatures or rainfall could be found. We conclude that the emissions reductions were too small in magnitude and time to have a significant effect on global climate, and that larger, sustained changes on a much longer timescale are required in order to have observable effects (Samset et al., 2020; Tebaldi et al, 2020). The CovidMIP protocol will be extended to include an additional "four-year blip" simulation so that future work can also consider the impact if lockdown restrictions were prolonged or recovery delayed due to new strains of the Coronavirus.

Based on what we have found we recommend further analysis would be fruitful in the following areas:

- *Effective radiative forcing (ERF) response to the emissions perturbations*: The global patterns of downwards SW radiation anomalies are very noisy in these simulations but the radiation signal would be improved in simulations with fixed-SSTs which reduce interannual variability in the climate system and allow quantification of the ERF due to the emission changes (Fiedler et al., 2020; Pincus et al., 2016). The CovidMIP protocol (Lamboll et al., 2020) defines additional fixed-SST simulations to isolate the effects of ozone, aerosols and even separate black carbon, organic carbon and sulfate aerosols. We recommend model groups perform these complementary simulations to allow the radiative effects of emissions reductions to be assessed more reliably.
- *Attribution of drivers of climate signals*: As part of DAMIP, this activity has a strong interest in performing single-forcing simulations to enable understanding of different drivers and causes of the climate changes seen. Large ensembles have been shown to be successful in detecting and attributing changes, for example, in recent southern hemisphere circulation changes to stratospheric ozone recovery (Banerjee et al., 2020). Similar techniques could be used here to separate the impacts of emissions reductions of GHGs and aerosols.
- *Longer term implications of emissions reductions and options for economic recovery*: Forster et al. (2020) compiled a set of hypothetical recovery scenarios based on moderate or strong green stimulus packages or a fossil-fuel stimulus rebound. The climate impacts by 2050 showed that how the world's economy recovers after 2020 can have profound impacts on our ability to meet long-term climate goals. Multi-model analysis of these simulations will enable clearer understanding of the threats and opportunities arising from the current situation.
- *Quantifying changes in extremes*: In addition to annual mean changes, the climate response in terms of extremes, such as daily maximum or minimum temperatures or daily precipitation rates, may also show important signals (Seneviratne & Hauser, 2020).
- *Influence on atmospheric circulation*: Studies have found a sensitivity of monsoons to changes in emissions of aerosols (Lau et al., 2017; Li et al., 2016; Meehl et al., 2008; Zhao et al., 2019). Analysis of these

changes in a multi-model study may be able to detect if COVID-19-related emissions reductions have had a detectable impact on monsoon circulations, especially over Asia.

- *Response and impacts of atmospheric composition*: The response of aerosols is detectable in this ensemble, but we have not yet explored the role of other chemically active components of the atmospheric composition. Especially, the role of ozone and its response to changes in emissions of precursors, is a key components of changes in air quality. Multiple studies have found increases in ozone in populated urban areas during lockdown (e.g., Keller et al., 2020), in contrast to a global decrease in tropospheric ozone (Weber et al., 2020). This MIP provides an opportunity to shed process-level understanding on these changes in a range of models of varying degrees of complexity with regards to atmospheric chemistry.

- *Impact on the global carbon cycle*: There is increasing interest in the ability to make predictions from one year to the next of changes in atmospheric CO_2 (Betts et al., 2016; Fransner et al., 2020; Lovenduski et al., 2019; Séférian et al., 2018; Spring & Ilyina, 2020). These studies require knowledge of natural causes of interannual variability, notable from ENSO (Watanabe et al., 2020), but they also require knowledge of up to date estimates of anthropogenic CO_2 emissions. These are normally expected to vary relatively little from year to year (Le Quéré et al., 2018) but expected impacts from COVID-19-related emissions reductions allow us to test out ability to forecast this most important metric of climate change, and whether external forcing can affect its variability (McKinley et al., 2020).

The SARS-Cov-2 pandemic of 2020 has created one of the biggest health and economic crises of recent history, but it also presents a remarkable opportunity to study how the climate system responds to changes in emissions of radiatively active species. From regional air quality to global climate this database of ESM outputs will enable advances in our understanding of how the climate system responds to short-term perturbations.

Data Availability Statement

This work used JASMIN, the UK's collaborative data analysis environment (http://jasmin.ac.uk, Lawrence et al., 2013). The authors are extremely grateful to the help and support of Martin Juckes, Alan Iwi, Ruth Petrie, Ag Stephens, Charlotte Pascoe at the Center for Environmental Data Analysis, Science and Technology Facilities Council, UK who facilitated the data sharing on JASMIN. CESM1 data can be accessed at https://zenodo.org/record/4521767. All other model data is published on the CMIP6 archive available via the Earth System Grid Federation. https://esgf-index1.ceda.ac.uk/search/cmip6-ceda/

References

Banerjee, A., Fyfe, J. C., Polvani, L. M., Waugh, D., & Chang, K. L. (2020). A pause in Southern Hemisphere circulation trends due to the Montreal Protocol. *Nature*. https://doi.org/10.1038/s41586-020-2120-4

Bao, R., & Zhang, A. (2020). Does lockdown reduce air pollution? Evidence from 44 cities in northern China. *Science of Total Environment*, *731*, 139052. https://doi.org/10.1016/j.scitotenv.2020.139052

Betts, R. A., Jones, C. D., Knight, J. R., Keeling, R. F., & Kennedy, J. J. (2016). El Nino and a record CO2 rise. *Nature Climate Change*, *6*, 806–810. https://doi.org/10.1038/nclimate3063

Boysen, L. R., Brovkin, V., Pongratz, J., Lawrence, D. M., Lawrence, P., Vuichard, N., et al. (2020). Global climate response to idealized deforestation in CMIP6 models. *Biogeosciences*, *17*, 5615–5638. https://doi.org/10.5194/bg-17-5615-2020

Buchwitz, M., Reuter, M., Noël, S., Bramstedt, K., Schneising, O., Fuentes Andrade, B., et al. (2020). Can a regional-scale reduction of atmospheric CO 2 during the COVID-19 pandemic be detected from space? A case study for East China using satellite XCO 2 retrievals. *Atmospheric Measurement Techniques Discussions*. https://doi.org/10.5194/amt-2020-386

Burrows, S. M., Maltrud, M., Yang, X., Zhu, Q., Jeffery, N., Shi, X., et al. (2020). The DOE E3SM v1.1 biogeochemistry configuration: description and simulated ecosystem-climate responses to historical changes in forcing. *Journal of Advances in Modeling Earth Systems*, *12*. https://doi.org/10.1029/2019MS001766

Chang, Y., Huang, R. J., Ge, X., Huang, X., Hu, J., Duan, Y., et al. (2020). Puzzling haze events in China during the Coronavirus (COVID-19) shutdown. *Geophysical Research Letters*, *47*, 1–11. https://doi.org/10.1029/2020GL088533

Chevallier, F., Zheng, B., Broquet, G., Ciais, P., Liu, Z., Davis, S. J., et al. (2020). Local anomalies in the column-averaged dry air mole fractions of carbon dioxide across the globe during the first months of the coronavirus recession. *Geophysical Research Letters*. https://doi.org/10.1029/2020GL090244

Diamond, M. S., & Wood, R. (2020). Limited regional aerosol and cloud microphysical changes despite unprecedented decline in nitrogen oxide pollution during the February 2020 COVID-19 shutdown in China. *Geophysical Research Letters*, *47*. https://doi.org/10.1029/2020GL088913

Döscher, R., Acosta, M., Alessandri, A., Anthoni, P., Arneth, A., Arsouze, T., et al. (2021). The EC-earth3 Earth system model for the climate model intercomparison project 6. *Geoscientific Model Development*, https://doi.org/10.5194/gmd-2020-446

Fiedler, S., Wyser, K., Rogelj, J., & van Noije, T. (2020). *Radiative effects of reduced aerosol emissions during the COVID-19 pandemic and the future recovery*. https://doi.org/10.1002/ESSOAR.10504704.1

Field, R., Hickman, J., Geogdzhayev, I., Tsigaridis, K., & Bauer, S. (2020). Changes in satellite retrievals of atmospheric composition over eastern China during the 2020 COVID-19 lockdowns. *Atmospheric Chemistry and Physics Discussions*. https://doi.org/10.5194/acp-2020-567

Filonchyk, M., Hurynovich, V., Yan, H., Gusev, A., & Shpilevskaya, N. (2020). Impact assessment of COVID-19 on variations of SO_2, NO_2, CO and AOD over east China. *Aerosol Air Quality Research*, *20*, 1530–1540. https://doi.org/10.4209/aaqr.2020.05.0226

Forster, P. M., Forster, H. I., Evans, M. J., Gidden, M. J., Jones, C. D., Keller, C. A., et al. (2020). Current and future global climate impacts resulting from COVID-19. *Nature Climate Change*. https://doi.org/10.1038/s41558-020-0883-0

Fransner, F., Counillon, F., Bethke, I., Tjiputra, J., Samuelsen, A., Nummelin, A., et al. (2020). Ocean biogeochemical predictions—initialization and limits of predictability. *Frontiers in Marine Science*, *7*. https://doi.org/10.3389/fmars.2020.00386

Gillett, N. P., Shiogama, H., Funke, B., Hegerl, G., Knutti, R., Matthes, K., et al. (2016). The Detection and Attribution Model Intercomparison Project (DAMIP~v1.0) contribution to CMIP6. *Geoscientific Model Development*, *9*, 3685–3697. https://doi.org/10.5194/gmd-9-3685-2016

Goldberg, D. L., Anenberg, S. C., Griffin, D., McLinden, C. A., Lu, Z., & Streets, D. G. (2020). Disentangling the impact of the COVID-19 lockdowns on urban NO2 from natural variability. *Geophysical Research Letters*. https://doi.org/10.1029/2020GL089269

Hajima, T., Watanabe, M., Yamamoto, A., Tatebe, H., Noguchi, M. A., Abe, M., et al. (2020). Development of the MIROC-ES2L Earth system model and the evaluation of biogeochemical processes and feedbacks. *Geoscientific Model Development*, *13*, 2197–2244. https://doi.org/10.5194/gmd-13-2197-2020

Hurrell, J. W., Holland, M. M., Gent, P. R., Ghan, S., Kay, J. E., Kushner, P. J., et al. (2013). The community earth system model: A framework for collaborative research. *Bulletin of the American Meteorological Society*, *94*, 1339–1360. https://doi.org/10.1175/BAMS-D-12-00121.1

Jones, C. D., & Cox, P. M. (2005). On the significance of atmospheric CO2 growth rate anomalies in 2002-2003. *Geophysical Research Letters*, *32*. https://doi.org/10.1029/2005GL023027

Kawamiya, M., Hajima, T., Tachiiri, K., Watanabe, S., & Yokohata, T. (2020). Two decades of Earth system modeling with an emphasis on Model for Interdisciplinary Research on Climate (MIROC). *Progress of Earth Planetary Science*, *7*, 64. https://doi.org/10.1186/s40645-020-00369-5

Keller, C. A., Evans, M. J., Knowland, K. E., Hasenkopf, C. A., Modekurty, S., Lucchesi, R. A., et al. (2020). Global impact of COVID-19 restrictions on the atmospheric concentrations of nitrogen dioxide and ozone. *Atmospheric Chemistry and Physics Discussions*, 1–32. https://doi.org/10.5194/acp-2020-685

Lamboll, R. D., Jones, C. D., Skeie, R. B., Fiedler, S., Samset, B. H., Gillett, N. P., et al. (2020). Modifying emission scenario projections to account for the effects of COVID-19: protocol for Covid-MIP. *Geoscientific Model Development*, 1–20. https://doi.org/10.5194/gmd-2020-373

Lau, W. K. M., Kim, K. M., Shi, J. J., Matsui, T., Chin, M., Tan, Q., et al. (2017). Impacts of aerosol–monsoon interaction on rainfall and circulation over Northern India and the Himalaya Foothills. *Climate Dynamics*, *49*, 1945–1960. https://doi.org/10.1007/s00382-016-3430-y

Lawrence, B. N., Bennett, V. L., Churchill, J., Juckes, M., Kershaw, P., Pascoe, S., et al. (2013). Storing and manipulating environmental big data with JASMIN. In *2013 IEEE international conference on big data* (pp. 68–75). IEEE. https://doi.org/10.1109/BigData.2013.6691556

Le, T., Wang, Y., Liu, L., Yang, J., Yung, Y. L., Li, G., et al. (2020). Unexpected air pollution with marked emission reductions during the COVID-19 outbreak in China. *Science*, *369*, 702–706. https://doi.org/10.1126/science.abb7431

Le Quéré, C., Andrew, R. M., Friedlingstein, P., Sitch, S., Hauck, J., Pongratz, J., et al. (2018). Global Carbon Budget 2018. *Earth System Science Data*, *10*, 2141–2194. https://doi.org/10.5194/essd-10-2141-2018

Le Quéré, C., Jackson, R. B., Jones, M. W., Smith, A. J. P., Abernethy, S., Andrew, R. M., et al. (2020). Temporary reduction in daily global CO2 emissions during the COVID-19 forced confinement. *Nature Climate Change*, *10*, 647–653. https://doi.org/10.1038/s41558-020-0797-x

Li, Z., Lau, W. K. M., Ramanathan, V., Wu, G., Ding, Y., Manoj, M. G., et al. (2016). Aerosol and monsoon climate interactions over Asia. *Reviews of Geophysics*, *54*, 866–929. https://doi.org/10.1002/2015RG000500

Lian, X., Huang, J., Huang, R., Liu, C., Wang, L., & Zhang, T. (2020a). Impact of city lockdown on the air quality of COVID-19-hit of Wuhan city. *The Science of the Total Environment*, *742*, 140556. https://doi.org/10.1016/j.scitotenv.2020.140556

Lian, X., Huang, J., Zhang, L., Liu, C., Liu, X., & Wang, L. (2020b). Environmental indicator for COVID-19 non-pharmaceutical interventions. *Geophysical Research Letters*, *48*(2), e2020GL090344. https://doi.org/10.1029/2020GL090344

Liu, Z., Ciais, P., Deng, Z., Lei, R., Davis, S. J., Feng, S., et al. (2020). Near-real-time monitoring of global CO2 emissions reveals the effects of the COVID-19 pandemic. *Nature Communications*, *11*, 5172. https://doi.org/10.1038/s41467-020-18922-7

Lovenduski, N. S., Bonan, G. B., Yeager, S. G., Lindsay, K., & Lombardozzi, D. L. (2019). High predictability of terrestrial carbon fluxes from an initialized decadal prediction system. *Environmental Research Letters*, *14*. https://doi.org/10.1088/1748-9326/ab5c55

Mauritsen, T., Bader, J., Becker, T., Behrens, J., Bittner, M., Brokopf, R., et al. (2019). Developments in the MPI-M Earth System Model version 1.2 (MPI-ESM1.2) and Its Response to Increasing CO2. *Journal of Advances in Modeling Earth Systems*, *11*, 998–1038. https://doi.org/10.1029/2018MS001400

McKinley, G. A., Fay, A. R., Eddebbar, Y. A., Gloege, L., & Lovenduski, N. S. (2020). External forcing explains recent decadal variability of the ocean carbon sink. *AGU Advances*, *1*. https://doi.org/10.1029/2019AV000149

Meehl, G. A., Arblaster, J. M., & Collins, W. D. (2008). Effects of black carbon aerosols on the Indian monsoon. *Journal of Climate*, *21*, 2869–2882. https://doi.org/10.1175/2007JCLI1777.1

Menut, L., Bessagnet, B., Siour, G., Mailler, S., Pennel, R., & Cholakian, A. (2020). Impact of lockdown measures to combat Covid-19 on air quality over western Europe. *The Science of the Total Environment*, *741*, 140426. https://doi.org/10.1016/j.scitotenv.2020.140426

Michou, M., Nabat, P., Saint-Martin, D., Bock, J., Decharme, B., Mallet, M., et al. (2020). Present-day and historical aerosol and ozone characteristics in CNRM CMIP6 simulations. *Journal of Advances in Modeling Earth Systems*, *12*. https://doi.org/10.1029/2019MS001816

Miyazaki, K., Bowman, K. W., Sekiya, T., Jiang, Z., Chen, X., Eskes, H., et al. (2020). Air quality response in China linked to the 2019 novel Coronavirus (COVID-19) mitigation. *Geophysical Research Letters*, *47*, e2020GL089252. https://doi.org/10.1029/2020GL089252

O'Neill, B. C., Tebaldi, C., van Vuuren, D. P., Eyring, V., Friedlingstein, P., Hurtt, G., et al. (2016). The Scenario Model Intercomparison Project (ScenarioMIP) for CMIP6. *Geoscientific Model Development*, *9*, 3461–3482. https://doi.org/10.5194/gmd-9-3461-2016

Ordóñez, C., Garrido-Perez, J. M., & García-Herrera, R. (2020). Early spring near-surface ozone in Europe during the COVID-19 shutdown: Meteorological effects outweigh emission changes. *The Science of the Total Environment*, *747*, 141322. https://doi.org/10.1016/j.scitotenv.2020.141322

Oshima, N., Yukimoto, S., Deushi, M., Koshiro, T., Kawai, H., Tanaka, T. Y., et al. (2020). Global and Arctic effective radiative forcing of anthropogenic gases and aerosols in MRI-ESM2.0. *Progress in Earth and Planetary Science*, *7*, 38. https://doi.org/10.1186/s40645-020-00348-w

Pincus, R., Forster, P. M., & Stevens, B. (2016). The Radiative Forcing Model Intercomparison Project (RFMIP): experimental protocol for CMIP6. *Geoscientific Model Development*, *9*, 3447–3460. https://doi.org/10.5194/gmd-9-3447-2016

Samset, B. H., Fuglestvedt, J. S., & Lund, M. T. (2020). Delayed emergence of a global temperature response after emission mitigation. *Nature Communications*, *11*, 3261. https://doi.org/10.1038/s41467-020-17001-1

Séférian, R., Berthet, S., & Chevallier, M. (2018). Assessing the decadal predictability of land and ocean carbon uptake. *Geophysical Research Letters*, *45*, 2455–2466. https://doi.org/10.1002/2017GL076092

Séférian, R., Berthet, S., Yool, A., Palmiéri, J., Bopp, L., Tagliabue, A., et al. (2020). Tracking Improvement in Simulated Marine Biogeochemistry Between CMIP5 and CMIP6. *Current Climatic Change Reports*. https://doi.org/10.1007/s40641-020-00160-0

Séférian, R., Nabat, P., Michou, M., Saint-Martin, D., Voldoire, A., Colin, J., et al. (2019). Evaluation of CNRM earth system model, CNRM-ESM2-1: Role of earth system processes in present-day and future climate. *Journal of Advances in Modeling Earth Systems*, *11*, 4182–4227. https://doi.org/10.1029/2019MS001791

Seland, Ø., Bentsen, M., Seland Graff, L., Olivié, D., Toniazzo, T., Gjermundsen, A., et al. (2020). The Norwegian Earth System Model, NorESM2 – Evaluation of theCMIP6 DECK and historical simulations. *Geoscientific Model Development Discussions*, 1–68. https://doi.org/10.5194/gmd-2019-378

Sellar, A. A., Jones, C. G., Mulcahy, J., Tang, Y., Yool, A., Wiltshire, A., et al. (2019). UKESM1: Description and evaluation of the UK Earth System Model. *Journal of Advances in Modeling Earth Systems*, 11(12), 4513–4558. https://doi.org/10.1029/2019MS001739

Seneviratne, S. I., & Hauser, M. (2020). Regional climate sensitivity of climate extremes in CMIP6 versus CMIP5 multimodel ensembles. *Earth's Future*, *8*. https://doi.org/10.1029/2019EF001474

Sicard, P., De Marco, A., Agathokleous, E., Feng, Z., Xu, X., Paoletti, E., et al. (2020). Amplified ozone pollution in cities during the COVID-19 lockdown. *The Science of the Total Environment*, *735*, 139542. https://doi.org/10.1016/j.scitotenv.2020.139542

Silver, B., He, X., Arnold, S. R., & Spracklen, D. V. (2020). The impact of COVID-19 control measures on air quality in China. *Environmental Research Letters*, *15*. https://doi.org/10.1088/1748-9326/aba3a2

Skeie, R. B., Myhre, G., Hodnebrog, Ø., Cameron-Smith, P. J., Deushi, M., Hegglin, M. I., et al. (2020). Historical total ozone radiative forcing derived from CMIP6 simulations. *Npj Climate and Atmospheric Science*, *3*, 32. https://doi.org/10.1038/s41612-020-00131-0

Spring, A., & Ilyina, T. (2020). Predictability horizons in the global carbon cycle inferred from a perfect-model framework. *Geophysical Research Letters*, *47*. https://doi.org/10.1029/2019GL085311

Stevens, B., Fiedler, S., Kinne, S., Peters, K., Rast, S., Müsse, J., et al. (2017). MACv2-SP: A parameterization of anthropogenic aerosol optical properties and an associated Twomey effect for use in CMIP6. *Geoscientific Model Development*, *10*, 433–452. https://doi.org/10.5194/gmd-10-433-2017

Sussmann, R., & Rettinger, M. (2020). Can we measure a COVID-19-related slowdown in atmospheric CO2 growth? Sensitivity of total carbon column observations. *Remote Sensing*, *12*, 2387. https://doi.org/10.3390/RS12152387

Swart, N. C., Cole, J. N. S., Kharin, V. V., Lazare, M., Scinocca, J. F., Gillett, N. P., et al. (2019). The Canadian Earth System Model version 5 (CanESM5.0.3). *Geoscientific Model Development*, *12*, 4823–4873. https://doi.org/10.5194/gmd-12-4823-2019

Tebaldi, C., Debeire, K., Eyring, V., Fischer, E., Fyfe, J., Friedlingstein, P., et al (2020). Climate model projections from the scenario model intercomparison project (ScenarioMIP) of CMIP6. *Earth System Dynamics Discussion*. https://doi.org/10.5194/esd-2020-68

Thornhill, G., Collins, W., Olivié, D., Archibald, A., Bauer, S., Checa-Garcia, R., et al. (2020). Climate-driven chemistry and aerosol feedbacks in CMIP6 Earth system models. *Atmospheric Chemistry and Physics*, 1–36. https://doi.org/10.5194/acp-2019-1207

Tjiputra, J. F., Schwinger, J., Bentsen, M., Morée, A. L., Gao, S., Bethke, I., et al. (2020). Ocean biogeochemistry in the Norwegian Earth System Model version 2 (NorESM2). *Geoscientific Model Development*, *13*, 2393–2431. https://doi.org/10.5194/gmd-13-2393-2020

Tohjima, Y., Patra, P. K., Niwa, Y., Mukai, H., Sasakawa, M., & Machida, T. (2020). Detection of fossil-fuel CO2 plummet in China due to COVID-19 by observation at Hateruma. *Scientific Reports*, 1–9. https://doi.org/10.1038/s41598-020-75763-6

Turner, A. J., Kim, J., Fitzmaurice, H., Newman, C., Worthington, K., Chan, K., et al. (2020). Observed impacts of COVID-19 on urban CO2 emissions. *Geophysical Research Letters*, 2–10. https://doi.org/10.1029/2020GL090037

Venter, Z. S., Aunan, K., Chowdhury, S., & Lelieveld, J. (2020). COVID-19 lockdowns cause global air pollution declines. *Proceedings of the National Academy of Sciences of the USA*, *117*, 18984–18990. https://doi.org/10.1073/pnas.2006853117

Wang, H., Easter, R. C., Zhang, R., Ma, P., Singh, B., Zhang, K., et al. (2020a). Aerosols in the E3SM Version 1: New developments and their impacts on radiative forcing. *Journal of Advances in Modeling Earth Systems*, *12*. https://doi.org/10.1029/2019MS001851

Wang, P., Chen, K., Zhu, S., Wang, P., & Zhang, H. (2020b). Severe air pollution events not avoided by reduced anthropogenic activities during COVID-19 outbreak. *Resources, Conservation and Recycling*, *158*, 104814. https://doi.org/10.1016/j.resconrec.2020.104814

Watanabe, M., Tatebe, H., Koyama, H., Hajima, T., Watanabe, M., & Kawamiya, M. (2020). Importance of El Niño reproducibility for reconstructing historical CO2 flux variations in the equatorial Pacific. *Ocean Science*, *16*, 1431–1442. https://doi.org/10.5194/os-16-1431-2020

Weber, J., Shin, Y. M., Sykes, J. S., & Archer-nicholls, S. (2020). Minimal climate impacts from short-lived climate forcers following emission reductions related to the COVID-19 pandemic. *Geophysical Research Letters*, *47*(20), e2020GL090326. https://doi.org/10.1029/2020GL090326

Xu, K., Cui, K., Young, L. H., Hsieh, Y. K., Wang, Y. F., Zhang, J., et al. (2020). Impact of the COVID-19 event on air quality in central China. *Aerosol Air Quality Research*, *20*, 915–929. https://doi.org/10.4209/aaqr.2020.04.0150

Yang, Y., Ren, L., Li, H., Wang, H., Wang, P., Chen, L., et al. (2020). Fast climate responses to aerosol emission reductions during the COVID-19 pandemic. *Geophysical Research Letters*, *47*. https://doi.org/10.1029/2020GL089788

Yukimoto, S., Kawai, H., Koshiro, T., OSHIMA, N., Yoshida, K., Urakawa, S., et al. (2019). The meteorological research institute earth system model version 2.0, MRI-ESM2.0: Description and basic evaluation of the physical component. *Journal of Meteorological Society in Japan: Series II*, *97*, 931–965. https://doi.org/10.2151/jmsj.2019-051

Zangari, S., Hill, D. T., Charette, A. T., & Mirowsky, J. E. (2020). Air quality changes in New York City during the COVID-19 pandemic. *The Science of the Total Environment*, *742*, 140496. https://doi.org/10.1016/j.scitotenv.2020.140496

Zhao, A. D., Stevenson, D. S., & Bollasina, M. A. (2019). The role of anthropogenic aerosols in future precipitation extremes over the Asian Monsoon Region. *Climate Dynamics*, *52*, 6257–6278. https://doi.org/10.1007/s00382-018-4514-7

Zhao, Y., Zhang, K., Xu, X., Shen, H., Zhu, X., Zhang, Y., et al. (2020). Substantial changes in nitrogen dioxide and ozone after excluding meteorological impacts during the COVID-19 outbreak in Mainland China. *Environmental Science and Technology Letters*, *7*, 402–408. https://doi.org/10.1021/acs.estlett.0c00304

Ziehn, T., Chamberlain, M. A., Law, R. M., Lenton, A., Bodman, R. W., Dix, M., et al. (2020). The Australian Earth System Model: ACCESS-ESM1.5. *Journal of Southern Hemisphere Earth Systems Science*, *70*(1), 193–214. https://doi.org/10.1071/es19035